metals

MDPI

Article

Influence of Temperature Regimes of Synthetic Iron Smelting on Casting Production Efficiency

Viktor Alekseevich Kukartsev [1], Alina Igorevna Trunova [1], Vladislav Viktorovich Kukartsev [2,3,4], Vadim Sergeevich Tynchenko [4,5,6], Sergei Olegovich Kurashkin [4,5,7,*], Kirill Aleksandrovich Bashmur [6], Yadviga Aleksandrovna Tynchenko [7,8], Roman Borisovich Sergienko [9] and Sergei Vasilievich Tynchenko [10,11]

1 Department of Materials Science and Materials Processing Technology, Polytechnical Institute, Siberian Federal University, 660041 Krasnoyarsk, Russia
2 Department of Informatics, Institute of Space and Information Technologies, Siberian Federal University, 660041 Krasnoyarsk, Russia
3 Department of Information Economic Systems, Institute of Engineering and Economics, Reshetnev Siberian State University of Science and Technology, 660037 Krasnoyarsk, Russia
4 Scientific and Educational Center "Artificial Intelligence Technologies", Bauman Moscow State Technical University, 105005 Moscow, Russia; vadimond@mail.ru (V.S.T.)
5 Information-Control Systems Department, Institute of Computer Science and Telecommunications, Reshetnev Siberian State University of Science and Technology, 660037 Krasnoyarsk, Russia
6 Department of Technological Machines and Equipment of Oil and Gas Complex, School of Petroleum and Natural Gas Engineering, Siberian Federal University, 660041 Krasnoyarsk, Russia
7 Laboratory of Biofuel Compositions, Siberian Federal University, 660041 Krasnoyarsk, Russia
8 Department of Systems Analysis and Operations Research, Reshetnev Siberian State University of Science and Technology, 660037 Krasnoyarsk, Russia
9 Machine Learning Department, Gini Gmbh, 80339 Munich, Germany
10 Department of Digital Control Technologies, Institute of Business Process Management, Siberian Federal University, 660041 Krasnoyarsk, Russia
11 Department of Computer Science and Computer Engineering, Institute of Computer Science and Telecommunications, Reshetnev Siberian State University of Science and Technology, 660037 Krasnoyarsk, Russia
* Correspondence: scorpion_ser@mail.ru; Tel.: +7-95-0973-0264

Abstract: The purpose of the foundry is to provide the consumer with blanks for general machine-building (special) purposes which are as close as possible to the size of the future part in full compliance with the requirements. The competitiveness of these products is primarily dependent on the use of efficient and reliable smelting equipment which meets the necessary cost. The replacement of high-value ironworks and ironworks iron with steel scrap using induction melting furnaces (ICFs) reduces the cost of producing synthetic cast iron. However, this results in temperatures greater than 1500 °C, reduced lining stability and increased downtime of the smelter. As a result of the research carried out, a technology for the use of quartzite is proposed. Thereby, the purpose of this work is to establish temperature regimes for the smelting of synthetic pig iron, allowing the use in metal filling up to 70–90% of steel scrap; this leads to a reduction in the cost of purchasing bulk materials (depending on the brand of cast iron) up to 50% and, thus, increases the efficiency of synthetic cast iron smelting and castings production in general. After removal of the original moisture and the subsequent sintering of the manufactured lining, it provides the possibility of melting using the melting temperatures 1550–1600 °C. It increases the efficiency of the operation of the melting furnaces and eliminates the consumption of the ironworks and the melting of the cast iron in the blast furnace, as well as the cost of the lost alloy. As a result, metallurgical production will be able to reduce the volume of production and supply of cast iron for ironworks, which will improve their environmental situation during the production and processing of necessary raw materials.

Keywords: acid lining; metallurgical resources; metal filling; induction crucible oven; lining resistance; production efficiency; synthetic cast iron; temperature melting modes

check for updates

Citation: Kukartsev, V.A.; Trunova, A.I.; Kukartsev, V.V.; Tynchenko, V.S.; Kurashkin, S.O.; Bashmur, K.A.; Tynchenko, Y.A.; Sergienko, R.B.; Tynchenko, S.V. Influence of Temperature Regimes of Synthetic Iron Smelting on Casting Production Efficiency. *Metals* **2023**, *13*, 1234. https://doi.org/10.3390/met13071234

Academic Editor: Nikki Stanford

Received: 27 April 2023
Revised: 22 June 2023
Accepted: 3 July 2023
Published: 5 July 2023

Copyright: © 2023 by the authors. Licensee MDPI, Basel, Switzerland. This article is an open access article distributed under the terms and conditions of the Creative Commons Attribution (CC BY) license (https://creativecommons.org/licenses/by/4.0/).

1. Introduction

The acquisition of the market for its products is carried out using advanced technologies that allow greater profitability and efficiency to be achieved by reducing material costs and reducing the downtime of major production equipment. The technology of producing castings from synthetic cast iron, used in the charging of scrap steel, is economically and environmentally profitable. The environmental benefit of the proposed development is that it does not require the use of ironworks and blast furnaces, which consume up to 1.5–3 tons of iron ore, 0.5–0.7 tons of coke, 0.5–0.725–4 tons of fluxes, and 2500–3000 m^3 of air and 200 L of water. In addition, the technologies currently used to process the required mineral raw materials have resulted in the depletion of reserves and the production of toxic metallurgical waste that pollutes the environment [1,2]. The disadvantage of this technology is the need to substantially increase the carbon content of the melt, resulting in a substantial increase in the amount of carburizer (1 ton of alloy to 40 kg). Additionally, carburization must be carried out at elevated temperatures, which adversely affect the stability of the furnace lining [3]. This means that to smelt 1 ton of synthetic cast iron for metal filling using no more than 30% of steel scrap, 10–15 kg carburizer is required, and 90% of steel scrap requires at least 40 kg.

An induction furnace (ICF; Figure 1) is used for synthetic cast iron smelting.

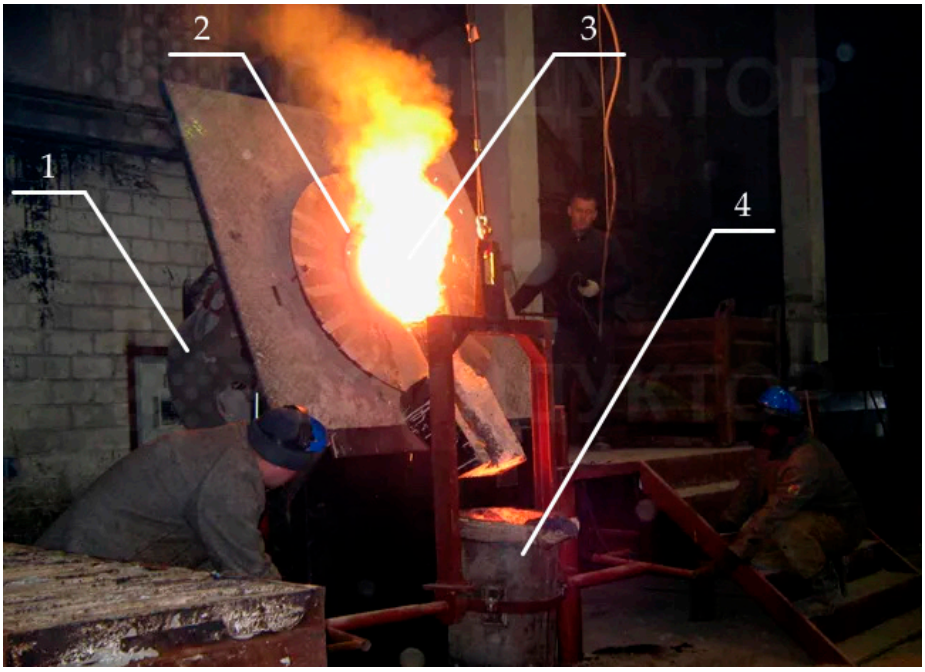


Figure 1. Picture of industrial-frequency induction crucible furnace at the moment of melting, where 1—furnace housing, 2—lining, 3—melt, and 4—casting ladle.

The industrial-frequency induction crucible furnace represents the basis of the production stock of the ironworks and, therefore, considerably affects the productivity of labor and its profitability. Efficient operation of the industrial furnace is the main objective of their reproduction. This is ensured by the use of technologies that provide versatility in the smelting of alloys, productivity, high lining resistance, and optimization of maintenance costs [4,5]. The industrial frequency induction smelter is designed for the smelting of synthetic cast iron using working modes of melting that do not exceed 1450 °C (a short increase to 1550 °C is permitted for carburizing). The quartzite, which is the basis of the furnace lining, allows it to withstand up to 350 melts.

The most important metallurgical process for melting synthetic cast iron in an induction electric furnace is the carburizing of the melt. This is because the technical and economic feasibility of using these furnaces is based on the use of cheap steel waste as the

charge material. The metal carburizing proceeds at a continuously changing temperature. For this reason, the original melt temperature should be no less than 1450 °C, and its reduction dramatically reduces the dissolution rate of the carbon. For synthetic cast iron smelting, up to 60% of the total carbon content (required) must be applied; for this reason, the melt must be held for 20–25 min at 1400–1450 °C. This ensures the formation of the necessary form and size of the graphite inclusions [6].

Thus, the synthetic cast iron smelting technology for ICF-2.5 kilns is as follows: After draining the finished metal at the specified temperature, a swamp is left in the furnace (1/3 of the volume of the crucible). During the discharge of and reduction in the volume of the alloy-filled crucible, the temperature in the furnace is reduced to 800–900 °C. Then, the furnace is refueled with a fresh charge and melted using power providing a temperature of 1300–1350 °C, followed by the carburizing and addition of ferroalloys with a temperature increase up to 1400–1470 °C. Then, the melt is extracted at a temperature of 1450–1500 °C, which is necessary for the formation of a favorable shape and size of the graphite, after which the temperature is reduced to 1400 °C, and the first portion of the melt is drained (800 kg) with inoculation by ferrosilicon FS-75 on the drain trough. The temperature in the furnace drops to 1000–1050 °C. When using a casting ladle with a capacity of 1 t, another casting ladle is drained without adding a fresh charge to avoid breaking the resultant chemical composition and the temperature before draining, raising it to 1400 °C. After draining, the temperature in the oven drops to 800–900 °C. Thus, the following temperature conditions are used for the production of synthetic cast iron:

- The lining is held at 1550 °C at the end of the sintering process;
- The optimum temperature range required for the carburization melt is 1400–1470 °C;
- The temperature range of the finished melt prior to its discharge is 1350–1450 °C, depending on the brand of the cast iron;
- The furnace cooling temperature range after the first batch of metal, no refill, is 1000–1050 °C;
- The cooling temperature range of the lining when the metal is completely drained and loaded with a new batch is 800–900 °C.

Additionally, the analysis of the use of charge materials in the smelting of synthetic cast iron of the mark CH20 according to GOST 1412-85 was carried out and was compared with the previous technology. For metal scrap containing 30% of steel scrap, the following materials were purchased: 15% (150 kg) of cast iron at 40 RUB/kg RUB 6000; 1% (10 kg) of ferromanganese and ferrosilicon at 50 RUB/kg in the amount of RUB 500; 30% (300 kg) of steel scrap at a price of 10 RUB/kg for the amount of RUB 3000, and 0.6% (0.6 kg) carburizer at a price of 3 RUB/kg for the amount of RUB 1.8 (the remaining mass of metal scrap consisted of the return of production and the liquid residue in the kiln, the notional cost of 1 ton of which is 50% for the liquid residue and 80% for the return of the cost of cast iron castings of the brand CH20 is 70 RUB/kg (330·35 = RUB 11,500 and 200·56 = RUB 11,200). The total cost was 32,201.8 RUB/liquid ton. For the smelting of 1 ton of liquid, when used in the meteor mill 88% of steel scrap, the costs were 1.5% ferrosol in the amount of RUB 750 100 kg liquid residue at a price of RUB 5000; 88% of steel scrap in the amount of RUB 8800; and 2% carburizer in the amount of RUB 6. The total cost of buying fresh materials amounted to RUB 14,556. The calculation uses the market value of the materials as of 2018–2019.

Thus, the novelty is as follows.

Temperature regimes used for synthetic cast iron smelting, with metal filling containing 30% scrap steel, cast iron scrap, casting iron, carburizing agent, ferroalloys, and return:

1. A total of 1400–1470 °C is the optimal melting point necessary for the carburizing of the melt;
2. A total of 1350–1450 °C—the temperature of the first portion of the melt, depending on the brand of cast iron;
3. A total of 1000–1050 °C—the temperature of the furnace cooling after the release of the second batch of metal, no refill;

4. A total of 800–900 °C—the cooling temperature of the lining when the metal is completely drained and its new batch is loaded.

Proposed (specified during the study) temperature regimes for the smelting of synthetic cast iron, using metal filling containing 70–90% steel scrap, carburizing agent, and ferroalloys:

1. A total of 1550–1600 °C—melting mode, carburizing, alloying, and modifying operation;
2. A total of 1450–1470 °C—discharge of the first portion of the alloy;
3. A total of 1000–1025 °C—the temperature of the furnace cooling after the release of the second batch of metal, no refill;
4. A total 800–900 °C is the cooling temperature of the lining when the metal is completely drained and a new batch is loaded.

2. Problem Statement

Polymorphic transformations occur in quartzite, as first described by the Fenner scheme (diagram) shown in Figure 2 [7].

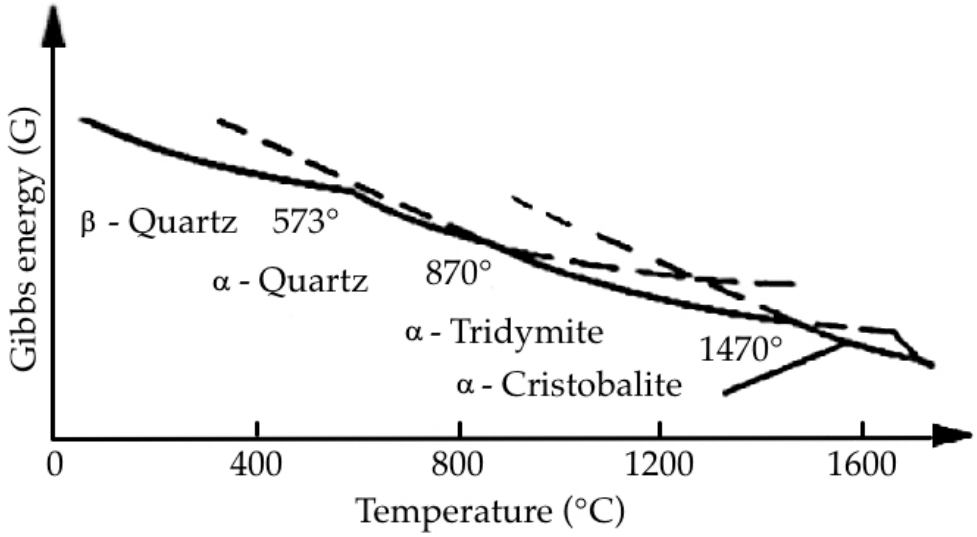


Figure 2. Silica polymorphism diagram at conditional coordinates of free energy–temperature (Fenner).

Similar processes should occur in quartzite, which is used for the manufacture of the furnace lining of ICFs and influences its durability [8–12]. The authors of [13] established the changes in the size of the quartzite crystal lattice, density of the elementary cell, and polymorphic transformations, which occurred under the following conditions:

- During moisture removal with different temperature modes;
- The temperature at the end of the sintering process of the lining;
- The temperature of the lining during loading of the next batch of bulk materials.

However, the parameters of the crystal lattice, which influence its changes during the action of temperature mode d_1 melting, also refer to the interdimensional distances, which also affects the stability of the lining [14]. The interdimensional distance is the d_1 value, a multiple of the distance between the nearest identical planes of atoms (ions) in the crystal, and indicates its health (Figure 3).

The quartzite pretreatment technology used to remove moisture also affects the lining stability and, therefore, the melting furnace operating efficiency [15]. The moisture present in the original quartzite and the nature of its further condition after drying and sintering of the lining [16–25] are also influential.

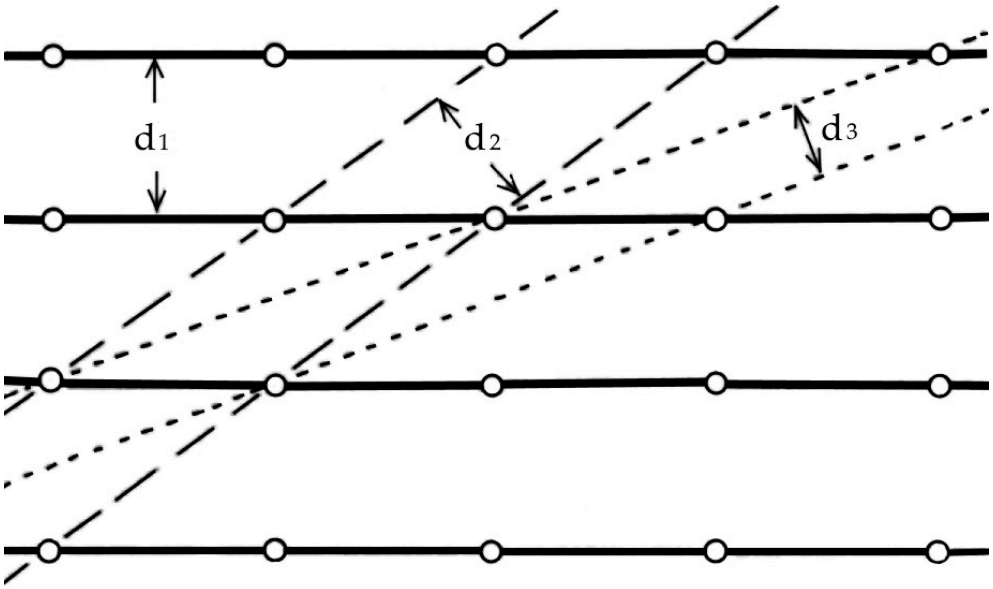


Figure 3. Diagram of various interdimensional distances d in crystal structure.

The efficiency of the smelter can be increased using metal filling consisting of 70–90% of steel scrap [26]. Synthetic grey cast iron, which is melted in induction furnaces during production in Russia, has been widely used abroad [27]. Its use requires an increase in the temperature necessary for high-quality carburizing of metal by 100–150 °C, because the carbon content must be increased three to four times and induces changes in the melting temperature (Figure 4) [28]. This exacerbates the problem of lining resistance, which reduces the efficiency of the melting furnace operation, as the downtime associated with relining also increases.

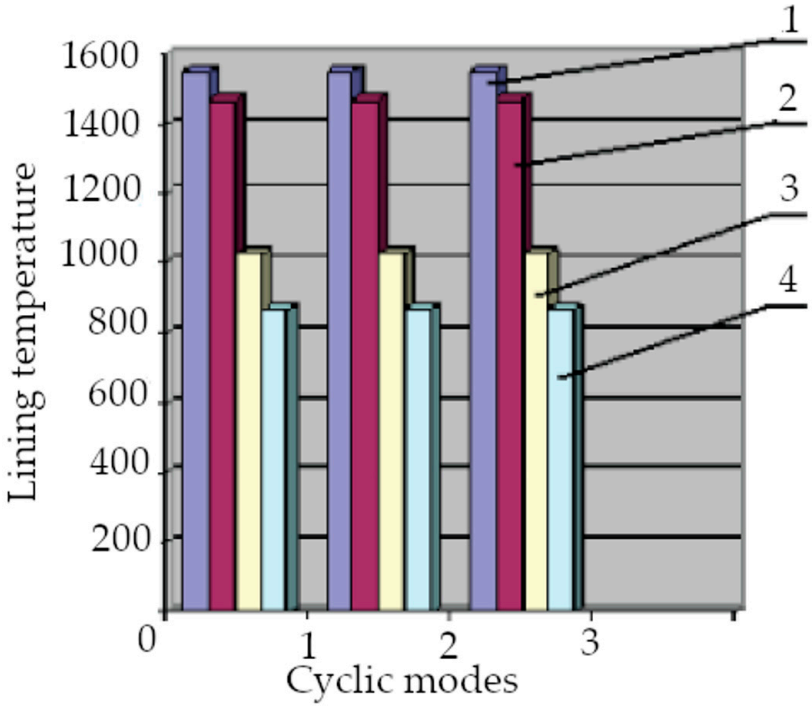


Figure 4. Technological smelting operations in the furnace ICF 2.5: 1—melting and Naugle-breeding mode, 1550–1600 °C; 2—discharging the first portion of metal, 1450–1470 °C; 3—discharging the second portion of metal, 1025 °C; 4—loading fresh metal filling, 800 °C.

These modes are maintained until the lining is completely worn out, i.e., until it is embossed. The application of high melting temperatures leads to a more intense reaction of the lining to the melt and substantially reduces its resistance [29]. Studies have shown the influence of melting temperatures above 1450 °C. If it increases by 100 °C, the resistance of the lining decreases to 180–200 melts [30]. The reason for this is the acceleration of the reaction $SiO_2 + 2C \rightarrow Si + 2CO \uparrow$. It causes rapid destruction (dissolution) of the lining. Because of this, the furnace is more frequently overfitted, resulting in increased downtime, material and energy waste, and ultimately reduces production efficiency. The use of other materials increases costs and provides less resistance. The corundum mass on the market costs RUB 70 per 1 kg; spinel-forming lining mass Coral CXL costs RUB 500 per 1 kg; the heat-resistant lining of induction furnaces for smelting alloy steel and cast iron at temperatures up to 1800 °C costs RUB 180 per 1 kg; dry sour quartzite Indastro Firebond MIX FS98 0.4 costs RUB 14 per 1 kg, and ground quartzite PCMVI 2 costs RUB 11 per 1 kg.

Several studies have been carried out to improve the properties of the acidic lining, allowing it to be used at temperatures above 1450 °C. The essence of these works lies in the use of various additional additives during the composition of the liner mixture. In most studies, these are additives in the form of calcium, iron, sodium, and chromium. Special mineralizers have also been proposed [30–38]. However, these methods have not been commercially applied.

Thus, the application of synthetic cast iron smelting temperature regimes, which ensure the efficiency of the smelter operation, depends directly on the stability of the acid quartzite-based lining and the financial cost of manufacturing it.

Until recently, the original document describing the phase transformation of quartzite when heated was the Fenner diagram (Figure 2): that is where the process of turning quartzite into trilimite begins, followed by the formation of a phase of cristobalite. Later, the findings of many studies refute this pattern. Other results from the heating of the quartzite are due to the imperfection of the physical and mechanical methods of research at the time. The X-ray crystallography method, introduced in the 1960s, revealed that during heating, cristobalite appears first and tridymite follows [39–46].

In industrial-frequency induction crucible furnaces, the melt is intensively mixed, which allows us to obtain melt with uniform structure and chemical composition and contributes to the process of intensive abrasion of the lining, which increases with the temperature. The acid lining, the main phase state of which is tridymite, has a high resistance, as it can maintain a constant volume for a long time and, therefore, ensures the efficient operation of the furnace itself [47]. The use of metal filling consisting of one steel scrap leads to the use of higher-temperature melting modes, as the required amount of naulerizing additive increases by 3–4 times. For this reason, another phase of quartzite is needed to withstand these conditions. This phase is cristobalite, which maintains its stability at temperatures 1470–1715 °C. Figure 5 shows a diagram of the lining layers after sintering at a temperature of 1550 °C, with the formation phases of a quartzite.

During the operation of the furnace, the process of corrosion of the lining occurs and the size of these zones changes. Their thicknesses, when adhered to the rules of operation of the furnace, decrease proportionally and polymorphic transformations of the quartzite occur in each zone, accompanied by a change in the proportion of the phases formed, especially for those that are sintered and semiwelded.

For this reason, this study was devoted to investigating the influence of advanced melting modes of synthetic cast iron on the phase state of quartzite, which ensures the operation efficiency of the furnace at operating temperatures above 1550–1600 °C using scrap metal from a scrap of steel.

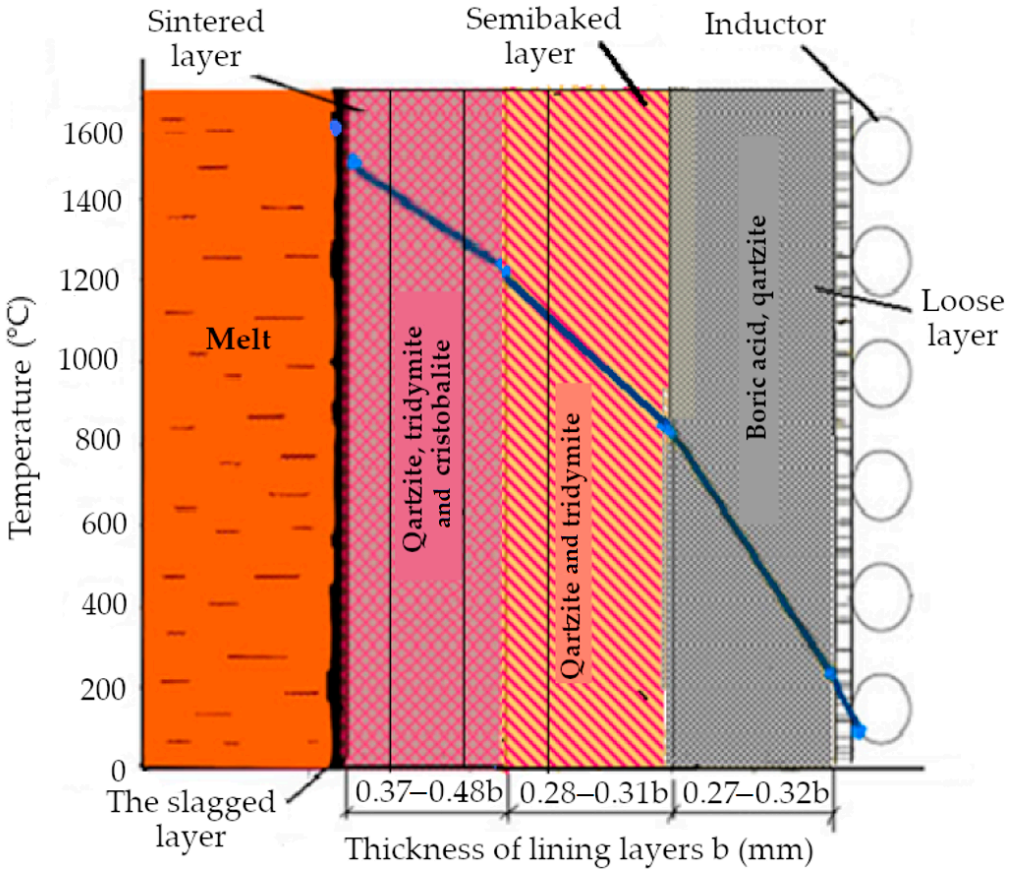


Figure 5. Arrangement of lining layers after sintering.

3. Materials and Methods

The material used was the Pervuralsky quartzite PKMVI-1 brand, with a humidity of 3.3%, supplied by Open Joint-Stock Company or JSC "DINUR" by TU1511-022-00190495-2003. The quartzite had a chemical composition as shown in Table 1 (retention of other impurities, such as CaO, MgO, TiO_2, P_2O_5, MnO, Na_2O, and K_2O, which are not always present). In addition, the enterprise was guaranteed the following grain composition, in mass shares:

- The remainder was on grid No. 02, including 6–13;
- The remainder on grid No. 3.2 was not more than 5;
- Pass through grid No. 05, including 52–59;
- Netting No. 01, 33–32.

Table 1. Chemical composition of PKMVI-1 quartzite.

Chemical Composition of PKMVI-1 Quartzite	Maintenance (%)									
	SiO_2	Al_2O_3	CaO	MgO	TiO_2	Fe_2O_3	P_2O_5	MnO	Na_2O	K_2O
According to TU	97.5	1.1	-	-	-	0.6	-	-	-	-
Spectrometer of dried at 200 °C	96.64	0.982	0.089	0.025	0.205	0.93	0.014	0.031	0.105	0.374

According to GOST 22552.7-2019 and TU 1511-022-00190495-2003, only the mass fraction in the mesh is required to be determined. At the moment, the pierced quartzite is scattered on the classifier (vibration) by fractions:

- 0.001–0.75 mm;
- 0.75–1.0 mm;
- 1.0–3.0 mm;
- 3.0 and more mm.

The study was conducted as follows:

1. The chemical composition of quartzite was determined, considering the presence of impurities;
2. The raw quartzite portion was heated to a temperature of 800 °C, given an exposure of 1 h, cooled to room temperature, and then subjected to subsequent heating to a temperature corresponding to the end of the process of sintering the lining (1550 °C) and subsequent temperatures, according to the melting temperature (twice) at each point to remove the card and determine the parameters of the crystal grille;
3. The next batch of raw quartzite was heated to a temperature of 200 °C, given an exposure of 1 h, cooled to room temperature, and then the same heating mode was performed as described in point 2.

The study temperature selection was based on the following:

- The approximate temperatures for the removal of free moisture are 200 and 800 °C;
- The melting mode, carburizing, alloying, and modifying operation temperature range is 1550–1600 °C;
- The temperature drainage range of the first portion of the alloy is 1450–1470 °C;
- The second alloy discharge temperature is 1025 °C;
- The loading temperature range of fresh scrap metal is 800–900 °C.

The chemical analysis was conducted via the fundamental parameter method using an X-ray fluorescence spectrometer Shimadzu XRF-1800. The device was equipped with collimators and a built-in digital camera; the rotation speed of the sample was 60 r/min.

The phase composition study was carried out using the diffractometer BRUKER D8 ADVANCE, which used the Bragg–Brentano focus and high-temperature camera HTK 16. In addition, an X-ray tube with a copper anode and a VÅNTEC-1 detector were used. The scan angle was 2Θ = 10–90, and the scan step was 0.007.

4. Results and Discussion

Since the formation of phases under the influence of temperature is influenced by the amount of impurities in the quartzite itself, the chemical composition of the quartzite was the first to be analyzed. The SiO_2 quantity was 96.64% instead of 97.5%, Al_2O_3 was 0.982 instead of 1.1%, Fe_2O_3 was 0.93% instead of 0.6%, which is significantly higher than under technical conditions, and the amount of unspecified impurities was 0.638%.

Further research was carried out using a diffractometer (BRUKER D8 ADVANCE). Figure 6 shows the diffractogram of the quartzite, with pretreatment at 800 °C, designed to remove moisture and then cooled to 30 °C. The lattice structure consists of elementary cells with properties given in the cards 01-083-2187 and 00-012-0708.

The structure of the quartzite lattice at 1550 °C is shown in Figure 7. The result obtained is similar to the result obtained for the Pervuralsky quartzite PKMVI-3 brand, which was made under the same conditions [48].

Figure 8 shows the diffractogram of quartzite, dried at 200 °C and cooled to 25 °C. The parameters of its structure were characterized using four varieties of elementary cells (cards 00-012-0708, 01-070-7344, 00-005-0490, and 01-083-2187).

The structure of the quartzite lattice at 1550 °C is shown in Figure 9. The result obtained is similar to the result obtained for the Pervuralsky quartzite PKMVI-3 brand, which was made under the same conditions [48].

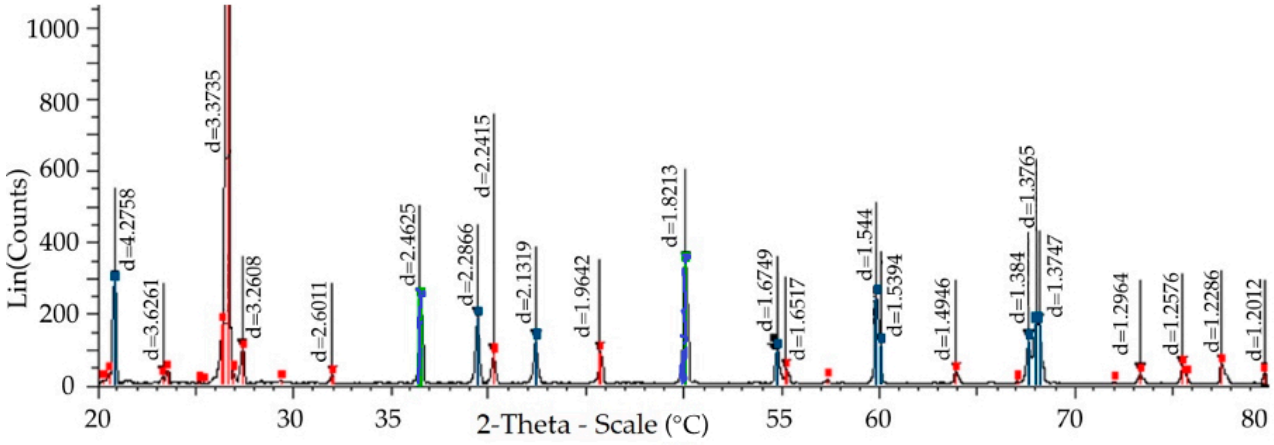


Figure 6. Quartzite diffractogram, taken at 30 °C, where ■—cells of the hexagonal quartzite characterized by card 00-012-0708 and ■—elementary cells of quartzite by card 001-083-2187 (remaining unspecified pixels and points are also red).

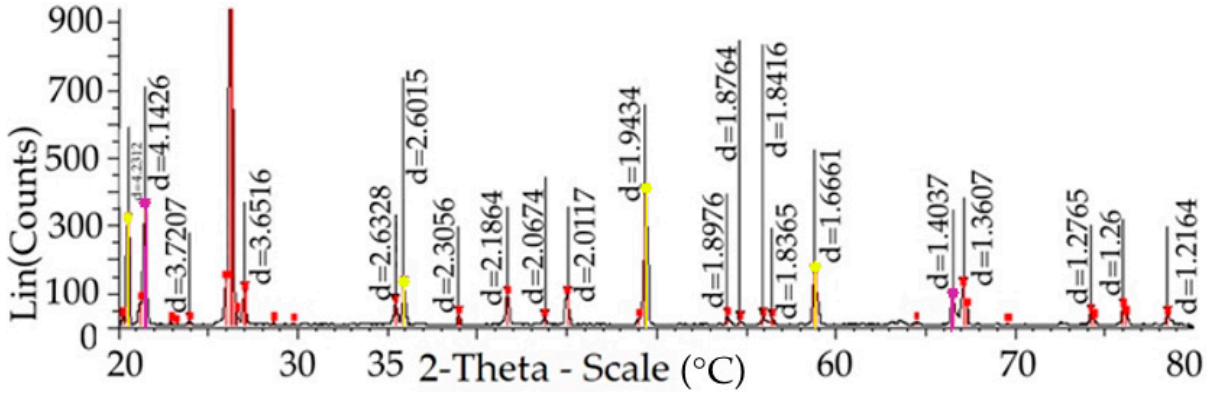


Figure 7. Quartzite diffractogram at 1550 °C, where ■—elementary cells of quartzite by card 01-085-0621; ■—tridymite cells by card 00-018-1170; and ■—quartzite cells by card 01-01-071 (remaining peaks and points in red).

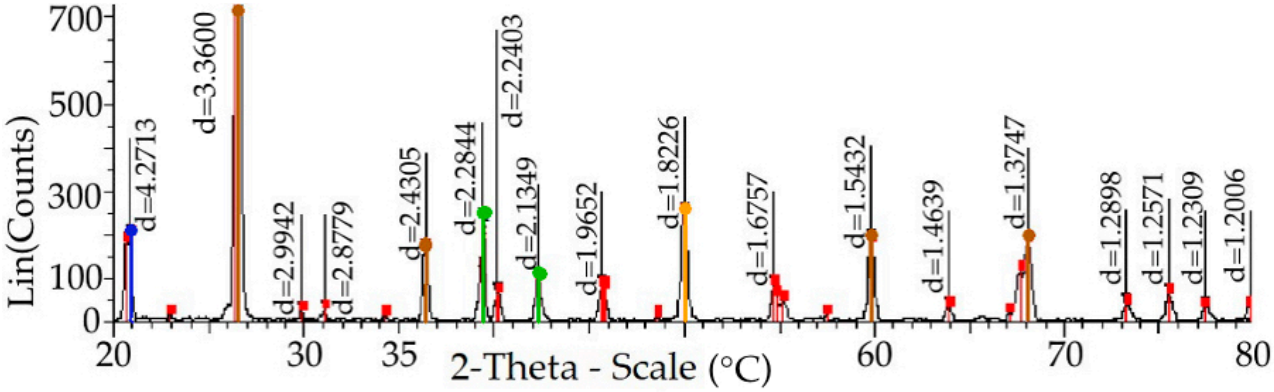


Figure 8. Diffractogram of structure of quartzite, dried at 200 °C and cooled to 25 °C, where ■—cells characterized by card 00-012-0708; ■—cells characterized by card 01-070-7344; ■—cells characterized by card 00-005-0490; ■—cells characterized by card 01-083-2187; and other cells—■.

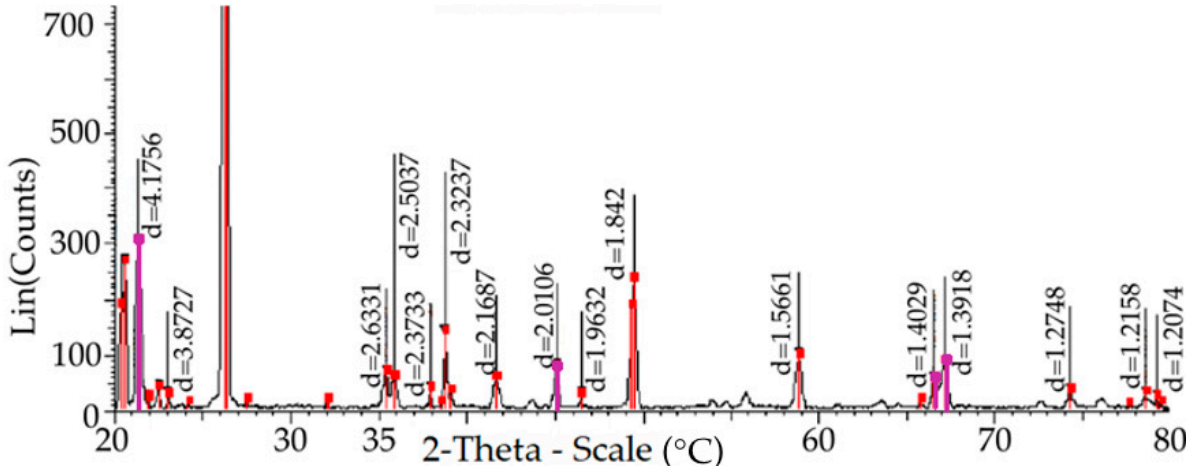


Figure 9. Diffractogram of quartzite at 1550 °C. Structure of quartzite consists of elementary cells of cristobalite, where ■—cards 00-011-0695 and 00-002-0278, and of quartzite, where ■—for the rest (card 01-071-0911). Remaining peaks and points are also red (■).

In order to decrypt the diffractograms obtained from the results of the research, the device software in the data bank, the cards describing the parameters of elementary cells were used. These cards of elementary cells of quartzite used in this study are presented in a previous study by the authors [48].

The cards helped to determine the number of elementary cells of each phase with a content of at least 5%. Their sum was taken for 100%. Then, the average values of the interplanar distances and all other parameters of the quartzite lattice structure were determined.

The values of the averaged parameters characterizing the structure of the quartzite lattice exposed to temperatures during the sintering process of the lining are presented in a previous study by the authors [48].

The numerator lists the averaged values d_{avg} (interglossy distance), D_{avg} (density), V_{avg} (volume), and M_{avg} (molar mass) of the quartzite grille processed at 200 °C, and the denominator at 800 °C.

The following phase changes occur in quartzite treated at 200°C during sintering: at 870 °C, its structure consists of 13% cristobalite, and the rest of the quartzite is hexagonal; at 1470 °C, the content of cristobalite changes to 16% and at 1550 °C it changes to 26%. In quartzite treated at 800 °C during sintering, the following phase changes occur: at 600 °C, its structure consists of 19% tridymite, and the rest of the quartzite is hexagonal; at 1470 °C; the tridymite content is 78%, and the hexagonal quartzite content is 22%; at 1550 °C, the content of tridymite increases to 82%, and the content of hexagonal quartzite and cristobalite is 9% each.

Considering the effect of the melting temperature conditions allowing the use of 90% or more of scrap steel in metal filling, the following phase changes were established in centimeters cubed, as shown in Figure 10.

Thus, at 1550 °C (after the first melting mode), the structure of quartzite treated at 900 °C was composed of elementary cells corresponding to 82% tridymite, 9% cristobalite, and 9% hexagonal quartzite. After exposure to the second temperature regime, 88% of the tridymite phase formed and 6% of the cristobalite and hexagonal quartzite phases formed.

The structure of quartzite at 1550 °C (after the first melting mode), subjected to temperature treatment at 200 °C, consisted of elementary cells corresponding to the phases of cristobalite in the amount of 26% and 74% of hexagonal quartzite. After the second temperature exposure, the fraction of cristobalite in the structure of quartzite was 35%, and the hexagonal quartzite was 65%.

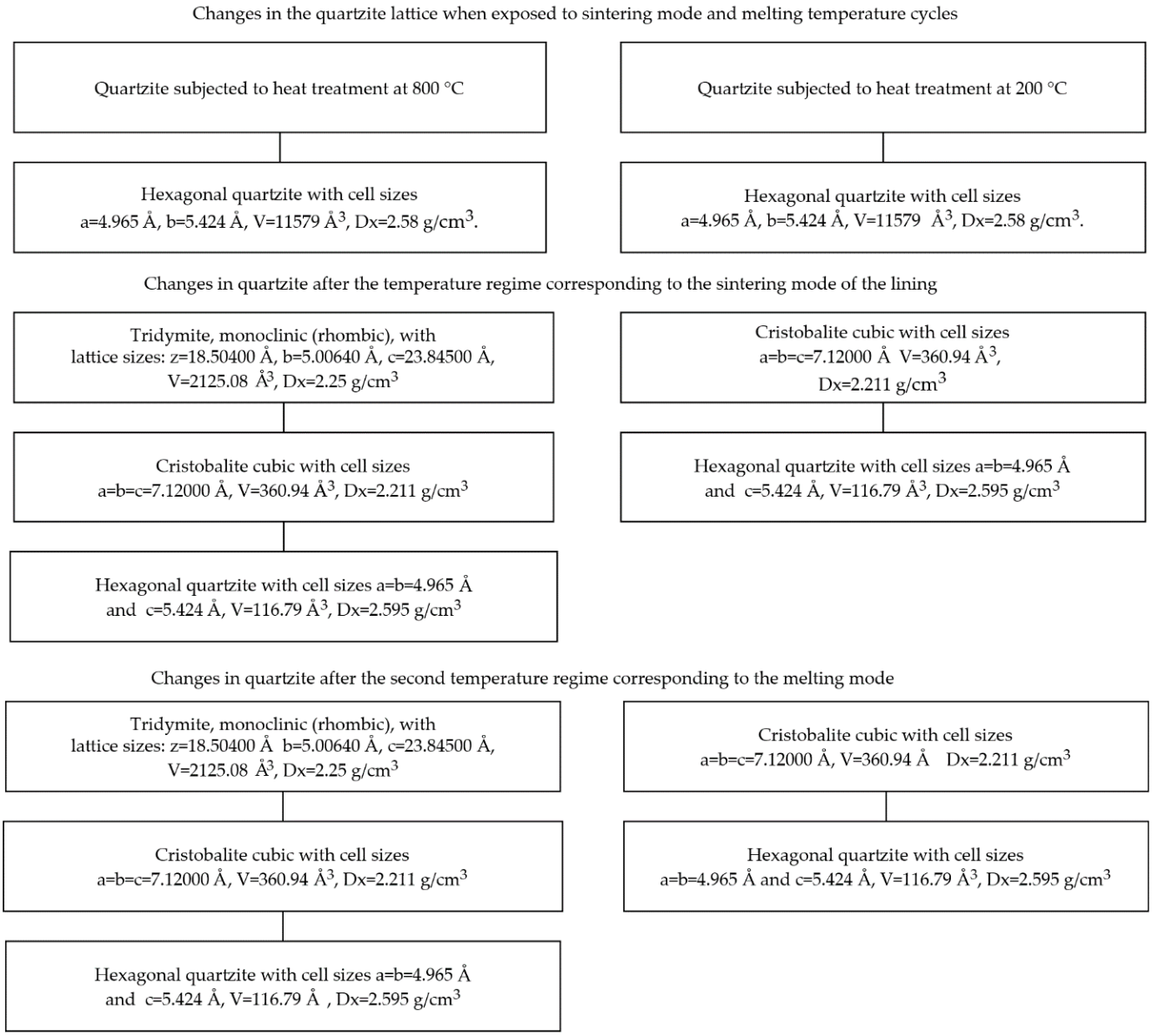


Figure 10. Phase changes in quartzite by melting temperature.

Cristobalite is known to be stable at 870–1470 °C and has a density of 2.3 g/cm^3 and a hardness of 6.5 units on the Moose scale. Cristobalite cubic is stable at a temperature of 1470–1715 °C, and has a hardness of 7.25 units and a density of 2.27 g/cm^2 [49]. Therefore, a sintered layer consisting of cristobalite and hexagonal quartzite has higher hardness and can withstand higher melting temperatures.

Consequently, the use of melting temperatures 1470–1570 °C requires the following new technology for the use of quartzite in the lining:

- Removing moisture using a temperature of 200 °C and then cooling;
- Ending the sintering process at 1550–1570 °C with an exposure of 2 h;
- Carrying out the first three to five melts with 1/3 of the capacity of the crucible and only then proceeding to the required melting mode.

Thus, by changing the temperature patterns of quartzite, a phase state that can withstand higher temperatures and higher thermal stability at melting temperatures above 1450 °C is required for the carburizing of synthetic cast iron fired from steel filling.

5. Discussion

The increased impurity content of the original material did not negatively affect the formation of phases under the influence of temperatures used to remove moisture and the subsequent sintering of the lining. Polymorphic transformations in quartzite occur in a pattern: quartzite hexagonal, tridymite at 600 °C, and cristobalite at 1550 °C. Additionally, for the formation of tridymite phase, no mineralizer was needed.

The lining, which has the dominant phase state in the form of tridymite, retains the constant volume and density at a temperature not exceeding 1450 °C.

The smelting of synthetic cast iron on a single scrap steel leads to an increase in the amount of material, increasing the carbon content, and requires the use of temperatures 1570–1620 °C. Only lining with a phase composition in the form of cristobalite can withstand them.

It has also been determined that tridymit, within a temperature range of 1200–1550 °C (the normal operating temperature range during smelting) allows volume changes in the limit of 9%, and 15% for cristobalite. This means that the cristobalite lining is more resistant to extreme temperature changes and has a higher level of hardness, which means greater resistance to abrasion of the actively mixing melt.

6. Conclusions

It has been established that the increase in the efficiency of the induction furnace of the industrial frequency, and, therefore, of the production as a whole, is achieved through the use of high-temperature regimes of synthetic cast iron smelting to reduce the cost of fresh materials by 40–45%. Thus, when using the ICFs -1 furnace for smelting 1 ton of liquid, 300 kg of cast iron and grey cast iron scrap is needed; when using metal filling only from steel scrap, these materials are not needed.

Temperature melting modes of 1550–1600 °C were determined. These are necessary for carburizing the alloy when using metal filling from a single steel scrap which requires the addition of a large amount of graphite–torus.

A phase study of quartzite exposed to high temperatures was conducted. It was found that the necessary re-presses of the melting can withstand the lining of the induction tiger furnace of industrial frequency, with subsequent operation resulting in the structure of the quartzite as cristobalite and hexagonal quartzite.

Thus, the technology of synthetic cast iron smelting in the ICFs proindustrial frequency furnace with acid lining consisting of quartzite and boric acid was developed.

Author Contributions: Conceptualization, V.A.K., V.V.K., V.S.T. and S.O.K.; methodology, V.A.K., V.V.K., V.S.T., S.O.K., K.A.B. and Y.A.T.; validation, K.A.B., Y.A.T., R.B.S., A.I.T. and S.V.T.; formal analysis, V.A.K., V.S.T., S.O.K., K.A.B., Y.A.T. and R.B.S.; investigation, V.S.T., S.O.K., K.A.B., Y.A.T., R.B.S., A.I.T. and S.V.T.; resources, V.V.K., V.S.T., S.O.K., K.A.B. and Y.A.T.; data curation, V.A.K., K.A.B., Y.A.T., R.B.S., A.I.T. and S.V.T.; writing—original draft preparation, V.A.K., V.V.K., V.S.T., S.O.K., K.A.B., Y.A.T., R.B.S., A.I.T. and S.V.T.; writing—review and editing, V.A.K., V.V.K. V.S.T., S.O.K., K.A.B., Y.A.T., R.B.S., A.I.T. and S.V.T.; visualization, V.V.K., V.S.T., S.O.K., R.B.S. and A.I.T.; supervision, V.S.T., S.O.K., K.A.B., Y.A.T., A.I.T. and S.V.T.; project administration, V.A.K., V.S.T., S.O.K., K.A.B., Y.A.T. and A.I.T.; All authors have read and agreed to the published version of the manuscript.

Funding: This research received no external funding.

Institutional Review Board Statement: Not applicable.

Informed Consent Statement: Not applicable.

Data Availability Statement: Not applicable.

Conflicts of Interest: The authors declare no conflict of interest.

References

1. Scobolev, D. *Encyclopaedia of Technologies. Evolution and Comparative Analysis of Resource Efficiency of Industrial Technologies*; D.O., S., Ed.; Renome: SPb, Russia, 2019; ISBN 978-5-00125-250-4.
2. Hopin, P.N. An Assessment of the Durability of Friction Couples with Solid Lubricant Coatings of Various Compositions Produced by Domestic and Foreign Manufacturers. *Mach. Build.* **2018**, *1*, 84–93. [CrossRef]
3. Konstantinos, I.V.; Charalambides, G. Market of High Purity Quartz Innovative Applications. *Procedia Econ. Financ.* **2015**, *24*, 734–742.
4. Kukartsev, V.V.; Antamoshkin, O.A. Combined Method of Decision-Making on Reproduction of Fixed Production Assets. *Probl. Mech. Eng. Autom.* **2011**, *1*, 56–60.
5. Onigbajumo, A.; Seidu, S.O.; Akinlabi, O.; Newton, I. Melting Time Prediction Model for Induction Furnace Melting Using Specific Thermal Consumption from Material Charge Approach. *J. Miner. Mater. Charact. Eng.* **2021**, *9*, 61–74.
6. Futas, P.J.A.; Pribulova, A.; Junakova, A.; Petrik, J.; Pokusova, M. The Study of Synthetic Cast Iron Quality Made from Steel Scrap. In Proceedings of the 18th International Multidisciplinary Scientific GeoConference SGEM 2018, Albena, Bulgaria, 2–8 July 2018; Volume 18, pp. 215–222.
7. Fenner, C.N. The various forms of silica and their mutual relations. *J. Wash. Acad. Sci.* **1912**, *2*, 471–480.
8. Zavertkin, A.S. Development of the Composition of the Lining of Induction Furnaces from Pervouralsk Quartzite and the Practice of Its Application. *Proc. Kola Sci. Cent. Russ. Acad. Sci.* **2015**, *44*, 532–534.
9. Grinchuk, P.S. Mathematical Modeling of Thermal Modes of Operation of Electric Resistance Furnaces. *Eng. Phys. J.* **2010**, *83*, 28–37.
10. Sassa, V.S. *Lining of Induction Melting Furnaces and Mixers*; Energoatomizdat: Moscow, Russia, 1983.
11. Kostyukova, A.P. Institutional Method as the Basis for Monitoring the Induction Melting Furnace. *Adv. Mod. Sci.* **2017**, *4*, 19–23.
12. Kukartsev, V.A. Application of Pervouralsky Quartzite in Acid Lining for Induction Iron-Smelting Furnaces. *Liteyshchik Russ.* **2012**, *2*, 35–37.
13. Chisamera, M.; Stan, S. Enhanced Quality in Electric Melt Grey Cast Irons Iulian Riposan. *ISIJ Int.* **2017**, *53*, 1683–1695.
14. Kukartsev, V.A.; Kukartsev, V.V.; Kukartsev, A.V. Cite as Effect of the Temperature Treatment of Quartzite on the Lining Resistance of Commercial-Frequency Induction Crucible Furnaces. *Refract. Ind. Ceram.* **2018**, *59*, 252–256. [CrossRef]
15. Kosenko, N.F.; Smirnova, M.A. Mechanostimulated Polymorphic Quartz Transitions. *Refract. Tech. Ceram.* **2012**, *7*, 7–13.
16. Potseluev, A.A.; Babkin, D.I.; Kotegov, V.I. Composition and Regularities of Gas Distribution in Quartz of the Kalgutinsky Rare Metal Deposit. *Proc. Tomsk Polytech. Univ.* **2005**, *308*, 36–42.
17. Hongwu, Z.; Songjiang, G.; Jijun, W.; Dandan, W.; Kuixian, W.; Wenhui, M. Effect of Quartz Crystal Structure Transformations on the Removal of Iron Impurities. *Hydrometallurgy* **2021**, *204*, 105715.
18. Fu, B.X.; Jacques, T.; Jacques, T. Fluid Inclusions in Coesitebearing Eclogites and Jadeite Quartzites at Schuanghe. *China J. Metamorph. Geol.* **2001**, *19*, 531–548. [CrossRef]
19. Kinelovskii, S.A. Model of Polymorphic Transformation in a Shock Wave. 2. Silica. *J. Appl. Mech. Tech. Phys.* **2021**, *62*, 214–223. [CrossRef]
20. Isaev, V.A.; Kharakhan, M.L. On the Role of Gas-Liquid Inclusions in the Process of Crystallization of Natural Quartz. *Min. Inf. Anal. Bull.* **2005**, *5*, 25–33.
21. Steinberg, M.V. Water and Hydrogen-Containing Groupings in Vein Quartz of Ural Deposits of Quartz Raw Materials. *Lithosphere* **2014**, *3*, 102–111.
22. Shabelansky, A.H.; Bernabe, Y.; Mok, U.; Evans, J.B. Temperature Influence on Permeability of Sioux Quartzite Containing Mixtures of Water and Carbon Dioxide. *Int. J. Rock Mech. Min. Sci.* **2014**, *70*, 546–551. [CrossRef]
23. Panasyuk, G.P.; Kozerozhets, I.V.; Voroshilov, I.L.; Privalov, V.I.; Ivakin, Y.D.; Danchevskaya, M.N. Water Forms on the Surface and in the Bulk of Silicon Dioxide. *Russ. J. Inorg. Chem.* **2021**, *66*, 724–730. [CrossRef]
24. Xin, C.; Zilong, Z.; Xueming, D. Water-Induced Variations in Dynamic Behavior and Failure Characteristics of Sandstone Subjected to Simulated Geo-Stress. *Int. J. Rock Mech. Min. Sci.* **2020**, *130*, 104339. [CrossRef]
25. Attinger, D.; Frankiewicz, C.; Betz, A.; Schutzius, T. Surface Engineering for Phase Change Heat Transfer: A review. *MRS Energy Sustain.* **2014**, *1*, E4. [CrossRef]
26. Kukartsev, V.A. Ncreasing the Resource of an Induction Crucible Furnace of Industrial Frequency at a Temperature above 1550 °C. *Technol. Mech. Eng.* **2014**, *1*, 5–6.
27. Edalati, K. Influence of SiC and FeSi Addition on the Characteristics of Gray Cast Iron Melts Poured at Different Temperatures. *Proc. Technol.* **2005**, *160*, 183–188. [CrossRef]
28. Zuno-Silva, J.; Bedolla-Jacuinde, A. Estudio a Nivel Laboratorio de La Degradación Atípica En Un Refractario Tipo SiO_2 Utilizado En Hornos de Inducción Laboratory Scale Study of Uncommon Degradation SiO_2 Refractories Used on Induction Furnaces. *Rev. Electron. Nov. Sci.* **2013**, *6*, 113–134.
29. Tgoupson, A.B.; Wennemer, M. Heat Capacities and Inversions in Tridymite, Cristobalite, and Tridymite-Cristobalite Mixedphases. *Am. Mineral.* **1979**, *64*, 1013–1026.
30. Kaibicheva, M.N. *Lining of Electric Furnaces*; Metallurgy: Moscow, Russia, 1975.
31. Masich, I.S.; Tyncheko, V.S.; Nelyub, V.A.; Bukhtoyarov, V.V.; Kurashkin, S.O.; Borodulin, A.S. Paired Patterns in Logical Analysis of Data for Decision Support in Recognition. *Computation* **2022**, *10*, 185. [CrossRef]

32. Kukartsev, V.A.; Cherepanov, A.I.; Kukartsev, V.V.; Tynchenko, V.S.; Kurochkin, S.O.; Tynchenko, V.V.; Sergienko, R.B.; Bashmur, K.A.; Boyko, A.A.; Bukhtoyarov, V.V. Influence of Moisture in Quartzite on the Lining Properties and Efficiency of Industrial-Frequency Induction Crucible Furnaces. *Metals* **2022**, *12*, 1515. [CrossRef]
33. Mass for the Printed Lining of Induction Furnaces. Available online: https://www.elibrary.ru/item.asp?id=39782161 (accessed on 21 February 2023).
34. Mikhalev, A.S.; Tynchenko, V.S.; Nelyub, V.A.; Lugovaya, N.M.; Baranov, V.A.; Kukartsev, V.V.; Sergienko, R.B.; Kurashkin, S.O. The Orb-Weaving Spider Algorithm for Training of Recurrent Neural Networks. *Symmetry Neurol. Int.* **2022**, *14*, 2036. [CrossRef]
35. Kukartsev, V.A.; Kukartsev, V.V.; Tynchenko, V.S.; Kurashkin, S.O.; Sergienko, R.B.; Tynchenko, S.V.; Panfilov, I.A.; Eremeeva, S.V.; Panfilova, T.A. Study of the Influence of the Thermal Capacity of the Lining of Acid Melting Furnaces on Their Efficiency. *Metals* **2023**, *13*, 337. [CrossRef]
36. Eskin, D.G. *Physical Metallurgy of Direct Chill Casting of Aluminum Alloys*; CRC Press: Boca Raton, FL, USA; Taylor & Francis: Oxfordshire, UK, 2008. Available online: https://www.taylorfrancis.com/books/mono/10.1201/9781420062823/physical-metallurgy-direct-chill-casting-aluminum-alloys-dmitry-eskin (accessed on 13 June 2023).
37. Kukartsev, V.; Mikhalev, A.; Stashkevich, A.; Moiseeva, K.; Kauts, I. Analysis of Data in Solving the Problem of Reducing the Accident Rate Through the Use of Special Means on Public Roads. In Proceedings of the 2022 IEEE International IOT, Electronics and Mechatronics Conference (IEMTRONICS), Toronto, ON, Canada, 1–4 June 2022; Institute of Electrical and Electronics Engineers (IEEE): Piscataway, NJ, USA, 2022; pp. 1–4.
38. Repinskiy, O.D.; Konyukhov, V.Y.; Bovkun, A.S.; Schupletsov, A.F. Improving the competitiveness of Russian industry in the production of measuring and analytical equipment. *J. Phys. Conf. Ser.* **2021**, *1728*, 012032. [CrossRef]
39. Novakovic, R.; Radic, S.M.; Ristic, M.M. Kinetics and Mechanism of Quartz-Tridymite Transformation. *NTERCERAM Interceram* **1986**, *35*, 29–30.
40. Kireev, T.; Kukartsev, V.; Pilipenko, A.; Rukosueva, A.; Suetin, V. Analysis of the Influence of Factors on Flight Delays in the United States Using the Construction of a Mathematical Model and Regression Analysis. In Proceedings of the 2022 IEEE International IOT, Electronics and Mechatronics Conference (IEMTRONICS), Toronto, ON, Canada, 1–4 June 2022; Institute of Electrical and Electronics Engineers (IEEE): Toronto, ON, Canada, 2022; pp. 1–5.
41. Breneman, R.C.; Halloran, J.W. Kinetics of Cristobalite Formation in Sintered Silica. *J. Am. Ceram. Soc.* **2014**, *9*, 2272–2278. [CrossRef]
42. Shchiptsov, V.V.; Perepelitsyn, V.A.; Grishenkov, E.E.; Enenko, V.P. Pervoural'skii and Karel'skii Quartzites for the Lining of Crucible-Type Induction Furnaces. *Refract. Ind. Ceram.* **2003**, *44*, 67–74. [CrossRef]
43. Kurashkin, S.; Bukhtoyarov, V.; Myrugin, A.; Bocharov, A.; Seregin, Y.; Rogova, D. Simulation Model of the Electron Beam Welding Process for the Formation of the Effective Technological Parameters during the Welding of Aerospace Structures. In Proceedings of the 2022 21st International Symposium Infoteh-Jahorina (Infoteh), East Sarajevo, Bosnia and Herzegovina, 16–18 March 2022; Institute of Electrical and Electronics Engineers Inc.: East Sarajevo, Bosnia and Herzegovina, 2022; pp. 1–5.
44. Nikiforova, E.M.; Eromasov, R.G.; Simonova, N.S.; Vasilyeva, M.N.; Taskin, V.Y. Phase Transformations in the Siliceous Rocks-Mineralizer System. *Mod. Probl. Sci. Educ.* **2012**, *1*, 218–219.
45. Rogova, D.; Kurashkin, S.; Tynchenko, V.; Shutkina, E.; Saidov, N.; Bocharov, A. Software System for Modeling Temperature Distribution During the Electron Beam Welding. In Proceedings of the 2022 IEEE International Conference on Design & Test of Integrated Micro & Nano-Systems (DTS), Cairo, Egypt, 6–9 June 2022; IEEE: Cairo, Egypt, 2022; pp. 1–6.
46. Li, W.; Xu, C.; Xie, A.; Chen, K.; Yang, Y.; Liu, L.; Zhu, S. Microstructure Study of Phase Transformation of Quartz in Potassium Silicate Glass at 900 °C and 1000 °C. *Crystals* **2021**, *11*, 1481. [CrossRef]
47. Jin, S.L.; Gruber, D.; Harmuth, H.; Soudier, J.; Meunier, P.; Lemaistre, H. Optimisation of Monolithic Lining Concepts of Channel Induction Furnace. *Int. J. Cast Met. Res.* **2014**, *27*, 336–340. [CrossRef]
48. Kukartsev, V.A.; Trunova, A.I.; Kukartsev, V.V.; Tynchenko, V.S.; Kurashkin, S.O.; Tynchenko, Y.A.; Vivián, I.F.; Bashmur, K.A. Increasing the Efficiency of Synthetic Iron Production by the Use of New Kit Lining. *Metals* **2023**, *13*, 1184. [CrossRef]
49. Ingham, J.P. Petrography of Geomaterials. *Q. J. Eng. Geol. Hydrogeol.* **2011**, *44*, 457–467. [CrossRef]

Disclaimer/Publisher's Note: The statements, opinions and data contained in all publications are solely those of the individual author(s) and contributor(s) and not of MDPI and/or the editor(s). MDPI and/or the editor(s) disclaim responsibility for any injury to people or property resulting from any ideas, methods, instructions or products referred to in the content.